2458 *Chem. Mater.* **2010,** *22,* 2458–2465
DOI:10.1021/cm903100a

CHEMISTRY OF MATERIALS
Article

Application of Magic-Angle Spinning NMR to Examine the Nature of Protons in Titanate Nanotubes

Dmitry V. Bavykin,*,† Marina Carravetta,‡ Alexander N. Kulak,† and Frank C. Walsh†

†*Materials Engineering and Energy Technology Research Groups, School of Engineering Sciences and* ‡*School of Chemistry, University of Southampton, Southampton SO17 1BJ, United Kingdom*

Received October 7, 2009. Revised Manuscript Received March 8, 2010

Systematic magic-angle spinning (MAS) ^{1}H NMR studies of protonated titanate nanotubes (produced by alkaline hydrothermal treatment of TiO_2 with NaOH) have revealed that there are several types of protons incorporated into their wall structure, including crystallographic water molecules and ion-exchangeable OH groups. Each type (a) has a characteristic chemical shift and (b) disappears at a different rate during annealing in air. The evolution of protons in titanate nanotubes during crystallographic and morphological transformation in the sequence $H_2Ti_3O_7 \cdot xH_2O$, $H_2Ti_3O_7$, $H_2Ti_6O_{13}$, TiO_2(B), TiO_2(anatase) during calcination, at temperatures from 140 to 500 °C, has been studied using MAS NMR and Raman spectroscopies together with thermogravimetric analysis (TGA), X-ray diffraction (XRD) and transmission electron microscopy (TEM) techniques. The irreversible disappearance of ion-exchangeable OH groups has been observed, even under low temperature treatment.

Introduction

Titanate nanotubes[1] have become the target of many studies in recent years because of their unique combination of physicochemical,[2] structural[3] and morphological[4] properties. They can be prepared in protonated (H-TiNT) and sodium-substituted (Na-TiNT) forms by hydrothermal treatment of powdered TiO_2 with a concentrated aqueous NaOH solution followed by washing and ion-exchange with acid or base. Originally discovered by Kasuga et al.,[5] tubular and fibrous nanostructures of titanates and TiO_2 show potential in a wide range of applications[6] including catalysis,[7,8] photocatalysis[9,10] and electrocatalysis, lithium batteries,[11,12] and solar cells[13,14] because of their open mesoporous morphology, high aspect ratio, ion-exchange properties[15,16] and moderate electrical conductivity. The abundance of titanate nanotubes with protons incorporated into the crystal structure is probably responsible for their high cationic conductivity[17] and capacity for hydrogen storage.[18,19] To improve their performance and understand the reasons affecting the efficiency of hydrogen storage in nanotubes, it is essential to relate the preparation conditions and post synthesis treatment to the nature and composition of protons in these materials.

The structure of H-TiNT is still disputed but it can be presented as a hydrated form of polytitanic acid having the general formula $H_2Ti_nO_{2n-m+1}(OH)_{2m} \cdot xH_2O$, where n, m, and x are numbers which depend on the preparation conditions and interpretation of the crystal structure. The structure of monoclinic trititanate ($H_2Ti_3O_7$) nanotubes suggested by Peng and co-workers[20] corresponds to the general formula with $n = 3$ and $m = 0$, whereas the structure of orthorhombic dititanate ($H_2Ti_2O_4(OH)_2$) nanotubes proposed by Jin et al[21] corresponds to $n = 2$ and

*To whom correspondence should be addressed. E-mail: d.bavykin@soton.ac.uk. Phone: + 44 2380598358. Fax: + 44 2380598754.

(1) Bavykin, D. V.; Walsh, F. C. *Titanate and Titania nanotubes: Synthesis, Properties and Applications*; Royal Society of Chemistry, Nanoscience and Nanotechnology: Cambridge, 2010.
(2) Bavykin, D. V.; Friedrich, J. M.; Walsh, F. C. *Adv. Mater.* **2006**, *18*, 2807–2824.
(3) Chen, Q.; Peng, L.-M. *Int. J. Nanotechnol.* **2007**, *4*, 44–65.
(4) Ou, H. H.; Lo, S. L. *Sep. Purif. Technol.* **2007**, *58*, 179–191.
(5) Kasuga, T.; Hiramatsu, M.; Hoson, A.; Sekino, T.; Niihara, K. *Langmuir* **1998**, *14*, 3160–3163.
(6) Bavykin, D. V.; Walsh, F. C. *Eur. J. Inorg. Chem.* **2009**, *8*, 977–997.
(7) Bavykin, D. V.; Lapkin, A. A.; Plucinski, P. K.; Friedrich, J. M.; Walsh, F. C. *J. Catal.* **2005**, *235*, 10–17.
(8) Idakiev, V.; Yuan, Z. Y.; Tabakova, T.; Su, B. L. *Appl. Catal., A* **2005**, *281*, 149–155.
(9) Yu, J.; Yu, H.; Cheng, B.; Zhao, X.; Zhang, Q. *J. Photochem. Photobiol. A: Chem.* **2006**, *182*, 121–127.
(10) Langhuang, H.; Zhongxin, S.; Yingliang, L. *J. Ceram. Soc. Jpn.* **2007**, *115*, 28–31.
(11) Armstrong, A. R.; Armstrong, G.; Canales, J.; Bruce, P. G. *J. Power Sources* **2005**, *146*, 501–506.
(12) Cheng, F.; Chen, J. *J. Mater. Res.* **2006**, *21*, 2744–2757.
(13) Ohsaki, Y.; Masaki, N.; Kitamura, T.; Wada, Y.; Okamoto, T.; Sekino, T.; Niiharab, K.; Yanagida, S. *Phys. Chem. Chem. Phys.* **2005**, *7*, 4157–4163.
(14) Hsiao, P. T.; Wang, K. P.; Cheng, C. W.; Teng, H. *J. Photochem. Photobiol. A: Chem.* **2007**, *188*, 19–24.
(15) Sun, X.; Li, Y. *Chem.—Eur. J.* **2003**, *9*, 2229–2238.
(16) Bavykin, D. V.; Walsh, F. C. *J. Phys. Chem., C* **2007**, *111*, 14644–14651.
(17) Thorne, A.; Kruth, A.; Tunstall, D.; Irvine, J. T. S.; Zhou, W. *J. Phys. Chem. B* **2005**, *109*, 5439–5444.
(18) Lim, S. H.; Luo, J.; Zhong, Z.; Ji, W.; Lin, J. *Inorg. Chem.* **2005**, *44*, 4124–4126.
(19) Bavykin, D. V.; Lapkin, A. A.; Plucinski, P. K.; Friedrich, J. M.; Walsh, F. C. *J. Phys. Chem. B* **2005**, *109*, 19422–19427.
(20) Chen, Q.; Du, G. H.; Zhang, S.; Peng, L. M. *Acta Crystallogr., Sect. B* **2002**, *58*, 587–593.
(21) Yang, J. J.; Jin, Z. S.; Wang, X. D.; Li, W.; Zhang, J. W.; Zhang, S. L.; Guo, X. Y.; Zhang, Z. J. *Dalton Trans.* **2003**, *20*, 3898–3901.

Published on Web 03/23/2010
© 2010 American Chemical Society

$m = 1$. The exact interpretation of the crystal structure of titanate nanotubes is problematic because of difficulties associated with the small size of the crystals and similarities in the X-ray diffraction patterns of various polytitanic acids. It is agreed, however, that protons occupy positions between the layers composed of TiO_6 octahedrons, in the multilayered wall structure of H-TiNT.[3]

The structure of H-TiNT involves several principal types of protons, namely, ion-exchangeable and non ion-exchangeable protons intrinsic to the crystal structure of titanates, as well as protons of crystallographic and physically adsorbed water molecules. The additional differences within these classes of protons can be associated with their location on the surface of, or intercalated between the layers inside, the nanotubes.[22] Such diversity in proton type in H-TiNT can be addressed by magic-angle spinning (MAS) NMR experiments. The ^{1}H-MAS NMR spectra of these systems consist of several overlapping peaks showing a chemical shift in the range from 2 to 12 ppm.[19]

Thermal treatment of H-TiNTs results in proton loss accompanied by crystallographic modifications which are eventually followed by the morphological transformation of nanotubes into nanorods. Most thermal transformation studies have involved temperatures between 300 and 600 °C.[23,24]

In this paper, we show for the first time that the loss of structural water in H-TiNT can be initiated at lower temperatures and monitored using NMR techniques, which has proved advantageous in identifying the nature of acid centers in zeolites during dehydration.[25] The nature of the protons in titanate nanotubes is systematically studied using ^{1}H MAS NMR spectroscopy of titanate nanotubes having different levels of ion-exchangeable H^+ and Na^+ ions. The effect of annealing at temperatures in the range 140 to 550 °C on the regularities of various types of proton disappearance is consistently connected with the water content, the total mass loss, the density change, and the modification of the crystal structure and the morphology of H-TiNTs. The degree of reversibility of ion-exchangeable proton loss during calcination has also been studied. Our results allow the controversy in determining the crystal structure of titanate nanotubes to be rationalized. Such a difference in interpretation can be associated with the loss of structural water in H-TiNT, even at low temperatures.

Experimental Details

Reagents. Titanium dioxide (anatase, TiO_2), sodium hydroxide (NaOH), potassium hydroxide (KOH), and hydrochloric acid (HCl), pure grade, were all obtained from Aldrich and were used without further purification.

Preparation of Protonated Titanate Nanotubes in Protonated and Sodium Forms. The preparation of titanate nanotubes was based on the alkaline hydrothermal method proposed by Kasuga et al.[5] and further developed in our laboratories toward a lower temperature, atmospheric pressure synthesis using KOH−NaOH mixtures[26] allowing a reflux method to be used. Two grams of titanium dioxide (anatase) was mixed with 240 cm^3 of 10 mol dm^{-3} NaOH and 10 cm^3 of 10 mol dm^{-3} KOH aqueous solutions, then placed in a PFA (perfluoroalkoxy polymer) round-bottom flask equipped with a thermometer, and refluxed at 106 °C for 4 days without stirring. The white, powdery titanate nanotubes produced were thoroughly washed with water until the washing solution achieved pH 7. To convert nanostructured titanates into their protonated form, the powder was then washed with an excess of 0.1 mol dm^{-3} HCl for over 30 min until a stable pH value of 2 was reached, followed by water washing to pH 5. The H-TiNT sample was dried in air at 140 °C overnight before being used for further experiments.

To exchange protons to sodium ions in the titanate nanotubes, 1 mol dm^{-3} NaOH solution was slowly added to a suspension of 1.5 g of H-TiNT in 150 cm^3 of water, and the pH was allowed to stabilize at the required value. After 30 min, the powder was washed with water and dried overnight at 140 °C. Three samples at pH = 2, 9, and 13 were prepared.

Measurement of the Kinetics of Ion-Exchange. Measurements of the kinetics of sodium ion-exchange into H-TiNT were adapted from our previous work.[16] A 0.1 g portion of a dry powder sample of H-TiNT was placed in the beaker, and 10 cm^3 of water was added. Under vigorous stirring, 0.05 cm^3 of 1 mol dm^{-3} NaOH solution was then quickly added. The dynamics of pH change were recorded using a Corning−250 ion analyzer equipped with a glass pH electrode at 25 ± 1 °C.

NMR Measurements. All ^{23}Na and ^{1}H NMR experiments were performed in a magnetic field of 14.1 T using a Bruker Avance II spectrometer equipped with a triple channel 2.5 mm probe at a spinning frequency of 28 kHz. The chemical shifts for ^{23}Na and ^{1}H were referenced to NaCl and adamantane, respectively.[27,28] A 6 mg portion of titanate nanotubes was placed in 2.5 mm zirconia rotors and annealed at a controlled temperature (140, 250, 350, and 450 °C) in a furnace for 24 h followed by cooling to 25 °C with a closed cap fitted. All ^{1}H NMR data were recorded with 64 scans using a Hahn echo sequence[29] and with an echo delay time of 35.7 μs, matching one rotor period. This time proved sufficient to successfully suppress the ^{1}H background. In the ^{1}H MAS NMR spectra, the sharp peaks near 1.4 ppm are attributed to artifacts, as verified by repeating the experiments on an empty rotor (data not shown). ^{23}Na NMR spectra were recorded with 128 scans via direct acquisition after annealing the sample at 140 °C.

Characterization of Samples. Transmission electron microscopy (TEM) images were obtained using a JEOL 3010-TEM transmission electron microscope. The powder sample was "dry" deposited onto a copper grid covered with a perforated carbon film. Raman spectra were recorded at room temperature (25 ± 2 °C) using a Renishaw 2000 spectrometer with HeNe laser (λ = 632.8 nm) excitation. Thermogravimetric analysis (TGA) curves were recorded using a PL-STA 1500 simultaneous

(22) Suetake, J.; Nosaka, A. Y.; Hodouchi, K.; Matsubara, H.; Nosaka, Y. *J. Phys. Chem. C* **2008**, *112*, 18474–18482.
(23) Morgado, E., Jr.; Jardim, P. M.; Marinkovic, B. A.; Rizzo, F. C.; Abreu, M. A. S.; Zotin, J. L.; Araujo, A. S. *Nanotechnology* **2007**, *18*, 495710–10.
(24) Lee, C. K.; Wang, C. C.; Lyu, M. D.; Juang, L. C.; Liu, S. S.; Hung, S. H. *J. Colloid Interface Sci.* **2007**, *316*, 562–569.
(25) Hunger, M. *Catal. Rev.* **1997**, *39*, 345–393.
(26) Bavykin, D. V.; Cressey, B. A.; Light, M. E.; Walsh, F. C. *Nanotechnology* **2008**, *19*, 275604–5.
(27) Hayashi, S.; Hayamizu, K. *Bull. Chem. Soc. Jpn.* **1989**, *62*, 2429–2430.
(28) Hayashi, S.; Hayamizu, K. *Bull. Chem. Soc. Jpn.* **1991**, *64*, 685–687.
(29) Ernst, R. R.; Bodenhausen, G.; Wokaun, A. *Principles of nuclear magnetic resonance in one and two dimensions*; Clarendon Press: Oxford, 1988.

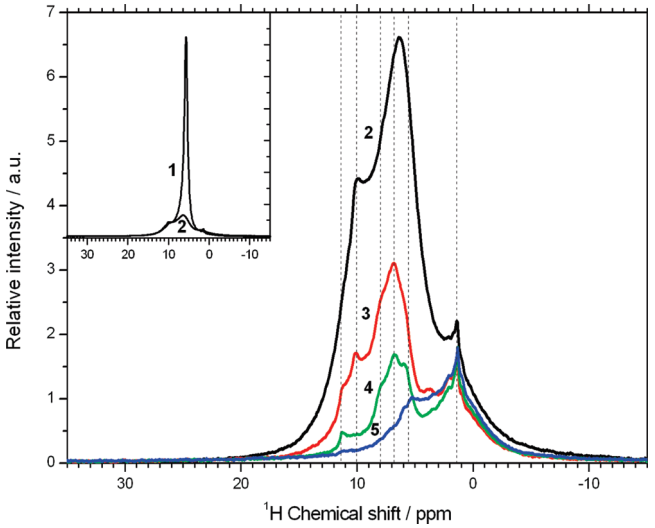

Figure 1. ^{1}H MAS NMR spectra of H-TiNT annealed at (2) 140 °C, (3) 250 °C, (4) 350 °C, and (5) 450 °C for 24 h. The inset shows the spectrum of H-TiNT saturated with water vapor of relative humidity 30% at 25 °C followed by drying in pure nitrogen for 3 h (1). Several peaks in the chemical shift region near 1.4 ppm are artifacts, i.e., signals from the NMR rotor.

analysis system. X-ray diffraction (XRD) patterns were obtained using a Bruker AXS D8 Discoverer X-ray diffractometer, equipped with Ni-filtered Cu Kα radiation (λ = 0.154 nm) and a graphite monochromator with an aluminum sample holder. The density of the nanotubes was determined by measuring the apparent sample volume, using helium as a filling gas, in a PCTPro 2000 gas adsorption apparatus.

Results and Discussion

When first discovered, titanate nanotubes were characterized as anatase.[1] However, systematic crystallographic and ion-exchange studies have since revealed the polytitanic nature of nanotubes.[3] The precise structure of titanate nanotubes is still disputed because of the difficulties associated with interpretation of data including the broadening of diffraction peaks caused by the small size of the structure and the insensitivity of crystallographic methods to low weight hydrogen atoms, resulting in a failure to locate their precise positions and population inside the crystal. The moderate thermal stability of titanate nanotubes can also give rise to poor reproducibility of experimental data.

Effect of Temperature on the Proton Composition in H-TiNT. At elevated temperatures, it is now agreed that at least three processes can occur in protonated titanate nanotubes, namely, dehydration, crystal structure transformation, and modification of morphology. All three processes occur simultaneously and each has a characteristic range of temperatures related to a particular phase transition.

Dehydration of H-TiNT is associated with removal of crystallographic water as well as combination of −OH groups forming water molecules.[23,24] Figure 1 shows ^{1}H MAS NMR spectra of H-TiNT annealed in air at different temperatures. The spectra contain several broad peaks, and the integrated signal intensities decrease at higher temperature, indicating the disappearance of protons from H-TiNT because of dehydration. Several characteristic proton resonance peaks can be identified at 11.4, 10.0, 7.9, 6.8, and 5.7 ppm with a typical line width in the range 1.5 to 3.5 ppm (see the Supporting Information, Table S1).

Table 1. ^{1}H MAS NMR Integral Area of Peaks and Amount of Water (y) at Different Chemical Shifts for Samples of Protonated Titanate Nanotubes Thermally Treated in the Air; Possible Stoichiometry of Titanate Nanotubes

		temperature/°C				
	chemical shift	25[a]	140	250	350	450
area at	11.4 ppm	0	0.994	0.845	0.445	0.132
	10.0 ppm	10.578	9.237	2.283	0.587	0
	7.9 ppm	9.116	10.967	4.654	1.117	0
	6.8 ppm	15.445	10.161	8.599	3.755	0
	5.7 ppm	83.370	15.241	1.452	0.981	4.717
	total	118.51	46.600	17.833	6.885	4.849
$y/\nu_{H2O}\nu_{TiO2}^{-1}$ at						
	11.4 ppm	0	0.0052	0.0044	0.0023	0.0007
	10.0 ppm	0.0549	0.0480	0.0119	0.0031	0
	7.9 ppm	0.0473	0.0570	0.0242	0.0058	0
	6.8 ppm	0.0802	0.0528	0.0447	0.0195	0
	5.7 ppm	0.4331	0.0792	0.0075	0.0051	0.0245[b]
	total	0.6155	0.2422	0.0927	0.0358	0.0252
TGA, wt %		100	92.49	89.97	88.47	88.13
crystal phase[c]						
$H_{2(1-z)}Ti_3O_{7-z}\cdot xH_2O$					TiO_2(B)	TiO_2
z		0.45	0.51	0.74	0.91	1
x		1.29	0.24	0.03	0	0

[a] Sample was saturated with water and then dried for 3 h at 25 °C. [b] The maximum of the peak was shifted to 5.1 ppm. [c] x and z were estimated for the trititanate structure of nanotubes.

The large peak widths in the ^{1}H spectra can be explained both by dipole−dipole interactions and by an intrinsic chemical shift spread, because of structural disorder within the sample, over a wide distribution of nanotube diameters. As a consequence, neither 2-D correlation experiments nor PMLG-type line narrowing experiments[30] have succeeded in improving the spectral resolution.

The progressive dehydration of the H-TiNT sample under heating results in significant changes in the ^{1}H spectra. The positions and the linewidths of all peaks exhibit minor non-systematic variations (see Supporting Information, Table S1) under dehydration; however, the integrals of the peaks decrease at very different rates (see Table 1), providing information on the nature of the protons for each peak. Figure 2 shows a deconvolution of the ^{1}H MAS NMR spectra of H-TiNT into several Lorentzian peaks. Since the exact nature and the mobility of the protons in titanate nanotubes are unknown, a Lorentzian function was assumed, since it enabled a better fit than a Gaussian one.

The fastest rate of decay is observed for the protons at 5.7 ppm, which is probably associated with removal of crystallographic water and (to a smaller extent) with physically adsorbed water molecules. Indeed, the chemical shift of physically adsorbed water has been reported at

(30) Vinogradov, E.; Madhu, P. K.; Vega, S. *Chem. Phys. Lett.* **2002**, *345*, 193–202.

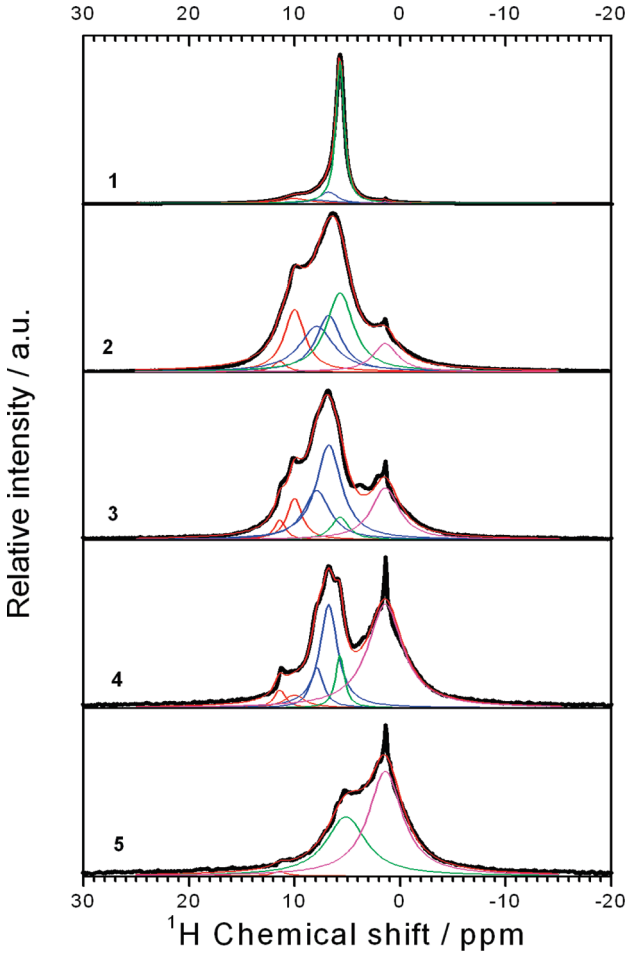

Figure 2. Deconvolution of ^{1}H MAS NMR spectra of H-TiNT into six superimposed Lorentzian shapes centered at 11.4, 10.0, 7.9, 6.8, 5.7, and 1.4 ppm. The samples were annealed at (1) 25 °C, (2) 140 °C, (3) 250 °C, (4) 350 °C, and (5) 450 °C for 24 h.

4.8 ppm[31] and at 4 ppm[17] for hydrated titanium(IV) oxide nanostructures, whereas the chemical shift of crystal water is close to 5.7 ppm (e.g., at 5.6 ppm[32]). It is also possible that most of the adsorbed water is removed during sample preparation. The process of incorporation/removal of crystallographic water is reversible at temperatures up to 140 °C. Following heating at 250 °C the integral intensity of the protons from crystallographic water is almost zero. After calcination at 450 °C, however, the intensity of this peak increases, and the peak shifts to 5.1 ppm, which is probably associated with surface OH groups of anatase (see Figure 2 and Table 1).

The decay rates of the other four resonance peaks under heating within the experimental error are in the order 10.0 ppm > 7.9 ppm > 6.8 ppm > 11.4 ppm. The recent ^{1}H MAS NMR studies of bulk ramdesite type crystals of $H_2Ti_3O_7$ have revealed two types of ion-exchangeable OH groups giving approximately equal intensity signals at 6 and 8 ppm.[33] The first one is related to less acidic protons, and the second one corresponds to the more acidic protons normally having resonance in weaker fields (larger chemical shift). The additional differentiations between protons can be achieved by the extensive surface of nanotubes resulting in a high proportion of surface to interlayer protons as observed for sodium ions.[22] The relatively large chemical shift of these acidic "non water" protons, may indicate the bridging nature of hydroxyl groups as observed in anatase at 6.7 ppm.[34] The protons at 11.4 ppm, which are most robust against dehydration under mild calcination conditions, have also been observed elsewhere in H-TiNT.[19] In contrast, non ion-exchangeable protons usually show resonance in a stronger field. For example, the protons in a perovskite type titanate $La_{2/3}TiO_{3-3x}(OH)_{3x}$ show resonances at 3.8 and 6.2 ppm.[35]

The area of the peaks can be correlated quantitatively with the amount of water in titanates, indicated y, which is defined as number of moles of H_2O over TiO_2 in the general formula $TiO_2 \cdot yH_2O$. The value of y can be determined from TGA data for water loss in H-TiNT (see the calibration in the Supporting Information, Figure S1). According to TGA, titanate nanotubes in their protonated form undergo complete dehydration at 500 °C, losing approximately 12% of their mass, which is equivalent to approximately 0.62 mols of water per mole of TiO_2 in titanates (see Figure 3a); 0.43 mols are accounted for crystallographic water and 0.19 mols correspond to the OH groups of titanates (see Table 1).

The exact crystal structure of titanate nanotubes is still under dispute; suggested structures include monoclinic trititanate ($H_2Ti_3O_7 \cdot xH_2O$),[20,36] orthorhombic dititanate ($H_2Ti_2O_4(OH)_2 \cdot xH_2O$),[21] and lepidocrocite-type ($H_{0.7}Ti_{1.827}\square_{0.175}O_{4.0} \cdot xH_2O$).[37,38] All of these structures can have a variable amount of crystallographic water and ion-exchangeable OH groups. During the dehydration initiated by thermal treatment of H-TiNT, both of these values decrease, resulting in a disturbance of the stochiometric composition. Thus, the general formula of H-TiNT can be expressed as $H_{2(1-z)}Ti_nO_{2n-m+(1-z)}(OH)_{2m} \cdot xH_2O$, where the variables x and z are associated with the amount of crystallographic water and ion-exchangeable OH groups, while n and m are associated with the type of crystal structure. It is important to relate the variables x, z, n, and m to experimentally determined amount of water y, which can be written as

$$y = \frac{1 + m + x - z}{n} \quad (1)$$

(31) Mogilevsky, G.; Chen, Q.; Kulkarni, H.; Kleinhammes, A.; Mullins, W. M.; Wu, Y. *J. Phys. Chem. C* **2008**, *112*, 3239–3246.
(32) Nag, A.; Lotsch, B. V.; Gunne, J. S.; Oeckler, O.; Schmidt, P. J.; Schnick, W. *Chem.—Eur. J.* **2007**, *13*, 3512–3524.
(33) Corcoran, D. J. D.; Tunstall, D. P.; Irvine, J. T. S. *Solid State Ionics* **2000**, *136*−*137*, 297–303.
(34) Cracker, M.; Herold, R. H. M.; Wilson, A. E.; Mackay, M.; Emeis, C. A.; Hoogendoorn, A. M. *J. Chem. Soc., Faraday Trans.* **1996**, *92*, 2791–2798.
(35) Bhuvanesh, N. S. P.; Bohnke, O.; Duroy, H.; Crosnier-Lopez, M. P.; Emery, J.; Fourquet, J. L. *Mater. Res. Bull.* **1998**, *33*, 1681–1691.
(36) Du, G. H.; Chen, Q.; Che, R. C.; Yuan, Z. Y.; Peng, L. M. *Appl. Phys. Lett.* **2001**, *79*, 3702–3704.
(37) Ma, R. Z.; Bando, Y.; Sasaki, T. *Chem. Phys. Lett.* **2003**, *380*, 577–582.
(38) Ma, R. Z.; Fukuda, K.; Sasaki, T.; Osada, M.; Bando, Y. *J. Phys. Chem. B* **2005**, *109*, 6210–6224.

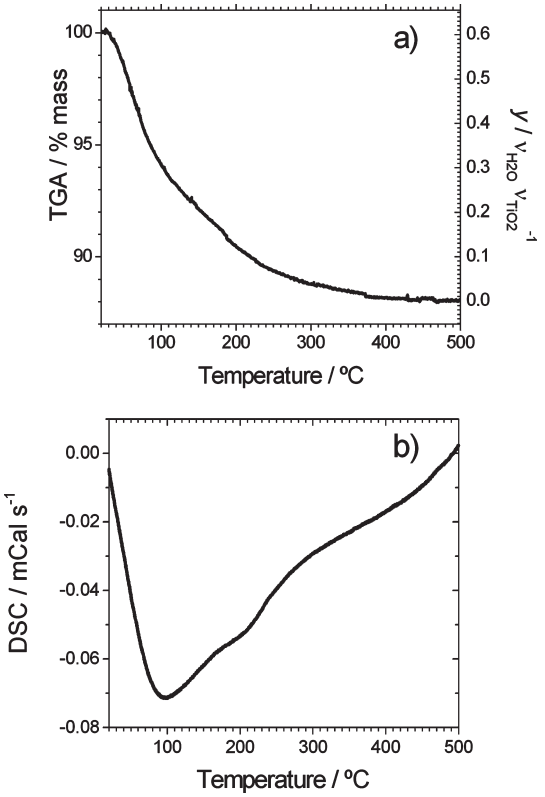

Figure 3. (a) TGA and (b) DSC curves of H-TiNT at a linear scan rate of 5 °C min^{-1}.

According to eq 1 the amount of water in orthorhombic dititanate, assuming no crystal water ($x = 0$) and no ion-exchangeable protons loss ($z = 0$), can reach $y = 1$. This value is much higher than 0.19 observed for the samples calcined at 140 °C (see Table 1). In contrast, both monoclinic trititanate and lepidocrocite-type titanates have a much smaller amount of water, namely, 0.33 and 0.192, respectively.

Although the observed amount of ion-exchangeable water in the H-TiNT sample calcined at 140 °C (0.19) is less than that in $H_2Ti_3O_7$ (0.33), such a trititanic structure cannot be discarded on that basis. It is possible that some of the ion-exchangeable OH groups in trititanate combine to form Ti−O−Ti surface groups and lose water under calcination at temperatures lower than 140 °C. Such a low stability of titanate nanotubes against dehydration is also consistent with rapid loss of ion-exchange capacity of H-TiNT under mild heating.

Figure 4 shows the kinetic curves for pH evolution after addition of a strong base into the suspension of H-TiNT calcined at various temperatures. For the blank solution of pure water, the addition of NaOH results in a very rapid increase of pH up to a value of 11.5 and an almost constant value within 60 min; in the case of nanotubes calcined at 140 °C, the initial rise of pH to almost 10 is followed by a slow decrease to 8. Such a large pH variation in the case of nanostructured titanates can be explained by the leaching of protons from the crystal structure of protonated titanates, which arises from the substitution of protons by sodium cations. The dynamics of pH change reflects the kinetic regularities of ion

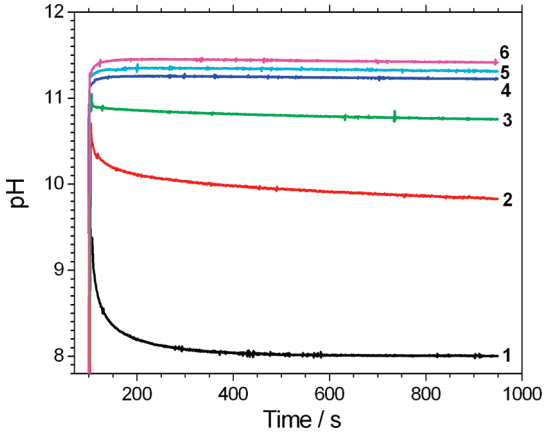

Figure 4. pH as a function of time following the addition of 0.05 cm^3 of 1 mol dm^{-3} NaOH to 10 cm^3 aqueous suspension of 0.1 g of H-TiNT calcined at (1) 140 °C, (2) 250 °C, (3) 350 °C, (4) 450 °C, and (5) 550 °C. (6) is the blank experiment without addition of nanotubes. The initial pH of water is about 4.5. pH was monitored at 25 °C.

transport in nanotubular titanates, and the amplitude of the pH variations is associated with the ion-exchange capacity of nanotubes, which depends on the number and accessibility of ion-exchangeable OH groups.[16]

An increase in the calcination temperature results in an irreversible decrease of ion-exchange capacity (see Figure 4) of nanotubes and a lower rate of ion transport inside the nanotube wall. This, in turn, is accompanied by the decrease of amount of ion-exchangeable protons (see Table 1). Such a dramatic decrease in the amount of ion-exchangeable OH groups in titanate nanotubes at temperatures lower than 250 °C is a new observation.

Previously,[23] dehydration of titanate nanotubes at temperatures below 250 °C was usually associated with the loss of crystallographic water rather than collapse of ion-exchangeable OH groups. This is also in agreement with good thermal stability of bulk $H_2Ti_3O_7$, which undergoes dehydration only at 245 °C.[39] Our current ^{1}H MAS NMR and ion-exchange data suggest a gradual disappearance of ion-exchangeable OH groups in H-TiNT even at lower temperatures (see Table 1). Surprisingly, such removal of ion-exchangeable OH groups (together with crystallographic water at temperatures below 250 °C) is accompanied by an increase in the apparent density of nanotubes measured using helium pycnometry (see Figure 5). The rise of density means that the decrease of nanotube mass, because of the water loss, is smaller than the volume decrease associated with the decrease of the interlayer spacing d_{200} in the wall of nanotubes[23] (see Figure 5). Indeed, the transport of ions in titanate nanotubes occurs along the axial direction of a nanotube between the layers of the wall.[16] The decrease of interlayer spacing is probably also responsible for the lower rate of ion-exchange (Figure 4) and for the smaller ion diffusion coefficient along the axis of the tube.

Figure 6 shows HRTEM images of protonated titanate nanotubes annealed at controlled temperatures. It is apparent that nanotubular morphology of H-TiNT is

(39) Feist, T. P.; Davies, P. K. *J. Solid State Chem.* **1992**, *101*, 275–295.

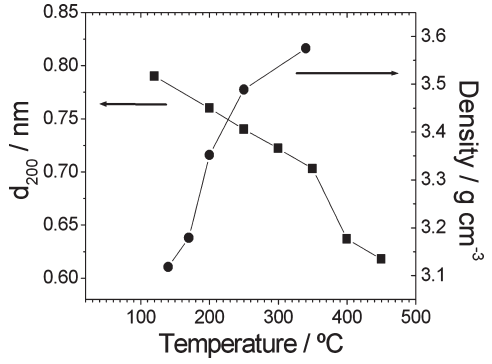

Figure 5. Apparent density of H-TiNT (●) and interlayer distance d_{200} in the nanotubes wall (■) as a function of calcination temperature. The value d_{200} was taken from reference 23.

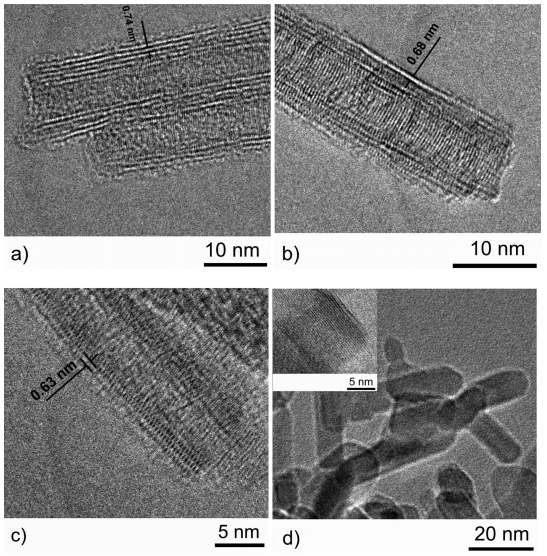

Figure 6. HRTEM images of H-TiNT annealed for 24 h at (a) 140 °C, (b) 250 °C, (c) 350 °C, and (d) 450 °C. The inset in (d) shows fringes of anatase (101) planes.

maintained until calcination temperatures reach 450 °C. At a higher temperature, the hollow cavity of the nanotube collapses forming rod-shaped objects consisting of the anatase phase of TiO_2 (Figure 6d). Thermal treatment of H-TiNT at temperatures in the range from 140 to 350 °C does not change the tubular shape of the titanates but results in a visible decrease in interlayer spacing. At temperatures above 250 °C, a topotactic transformation of $H_2Ti_3O_7$ to the intermediate phases of $H_2Ti_6O_{13}$ and $H_2Ti_{12}O_{25}$ may occur[23] followed by formation of the monoclinic TiO_2(B) phase.[40] Such crystallographic changes are in agreement with the irreversible decrease in ion-exchange capacity of H-TiNT at elevated temperatures (see Figure 4).

Raman spectroscopic data also confirm the disappearance of the titanate phase and formation of anatase during calcination (Figure 7). The temperature dependence of the Raman spectrum of H-TiNT is consistent

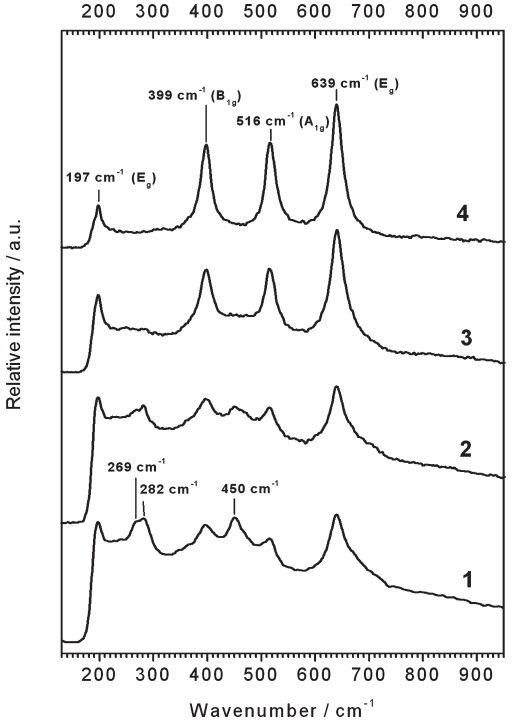

Figure 7. Raman spectra of H-TiNT calcined for 24 h at (1) 140 °C, (2) 250 °C, (3) 350 °C, and (4) 450 °C.

with recent in situ Raman studies.[41] The spectrum of initial protonated titanates shows a characteristic split peak at approximately 280 cm^{-1} and one at 450 cm^{-1}. The weak characteristic peaks of H-TiNT at higher energy (e.g., 665 cm^{-1} and 700 cm^{-1}) are masked by the strong signal from anatase impurities at 639 cm^{-1}. The characteristic signal from Ti−O−Na oscillations at 913 cm^{-1} is undetected, probably because of the small amount of sodium ions in the structure, which often occurs after substitution of sodium ions to protons.[42] At a calcination temperature above 450 °C, the Raman spectrum of the sample corresponds to that of pure anatase with characteristic allowed oscillation modes at 197 cm^{-1} (Eg), 399 cm^{-1} (B1g), 513 cm^{-1} (A1g), 519 cm^{-1} (B1g), and 639 cm^{-1} (Eg).[43]

Figure 8 shows the powder XRD pattern of H-TiNT calcined at different temperatures. The characteristic (200) reflection at about 10° shifts to larger angles at higher temperatures, indicating a decrease in the interlayer spacing in the titanate nanotube walls accompanied by removal of water. The structural changes in H-TiNT under calcination are similar to those reported elsewhere[23] and generally follow the sequence titanate → monoclinic TiO_2(B) → anatase.

Effect of Sodium Ion on the Proton Composition in H-TiNT. The titanate nanotubes are characterized by relatively good ion-exchange properties which allow the reversible exchange of protons to alkali metal ions

(40) Armstrong, G.; Armstrong, A. R.; Canales, J.; Bruce, P. G. *Chem. Commun*. **2005**, *19*, 2454–2456.
(41) Cortes-Jacome, M. A.; Ferrat-Torres, G.; Flores Ortiz, L. F.; Angeles-Chavez, C.; Lopez-Salinas, E.; Escobar, J.; Mosqueira, M. L.; Toledo-Antonio, J. A. *Catal. Today* **2007**, *126*, 248–255.
(42) Bavykin, D. V.; Friedrich, J. M.; Lapkin, A. A.; Walsh, F. C. *Chem. Mater*. **2006**, *18*, 1124–1129.
(43) Ohsaka, T. *J. Phys. Soc. Jpn*. **1980**, *48*, 1661–1668.

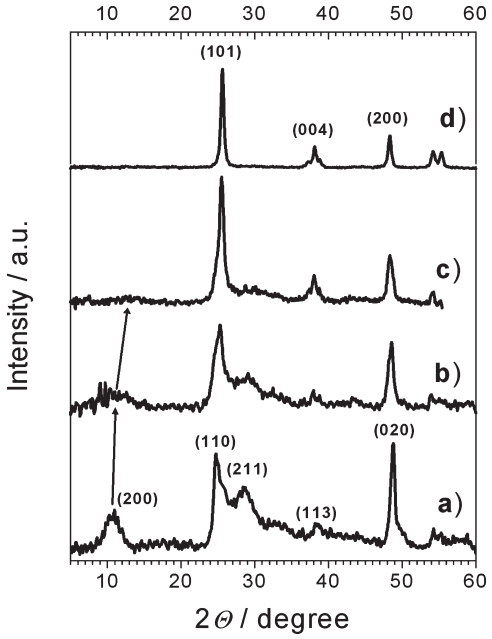

Figure 8. XRD patterns of H-TiNT calcined for 24 h at (a) 140 °C, (b) 250 °C, (c) 350 °C, and (d) 450 °C.

via the reaction:

$$Na^+ + H_2Ti_3O_7 \leftarrow \rightarrow H^+ + NaHTi_3O_7 \qquad (2)$$

. It is possible to identify the OH groups of titanates involved in reaction (2) by studying the ^{1}H MAS NMR spectra of titanate nanotubes having different amounts of ion-exchanged sodium. Stirring of the suspended H-TiNT in an aqueous solution of NaOH results in the equilibrium described by reaction (2), and the amount of sodium in the nanotubes can be controlled by adjusting the pH of the suspension.

Figure 9a shows ^{1}H MAS NMR spectra of titanate nanotubes suspended at pH 2, 9, and 13, followed by their calcination at 250 °C. Addition of sodium ions results in a lower intensity of peaks at 6.8, 7.9, 10.0, and 11.4 ppm confirming the ion-exchangeable nature of these protons. Partial substitution of H^+ to Na^+ does not alter their chemical shift or the line width of peaks within the margins of error (see the Supporting Information, Table S1 and Figure S2). This indicates a weak effect of the Na^+ ions on the local electronic structure near the exchangeable H^+, probably because of the large distance between them in the lattice of titanate nanotubes, resulting in weak interactions between ions.

The presence of crystallographic water in the structure of titanate nanotubes complicates the interpretation of ^{1}H MAS NMR spectra of titanate nanotubes suspended at pH 2, 9, and 13 followed by their calcination at 140 °C (Figure 9b). An increase in the amount of Na^+ in the nanotubes also results in a lower intensity of the proton peaks at 11.4 and 10.0 and a shift of the peak at about 6−7 ppm to higher field. The deconvolution of these spectra (see the Supporting Information, Figures S2 and S3) reveals that substitution of protons in titanate nanotubes by sodium ions results in a smaller signal from

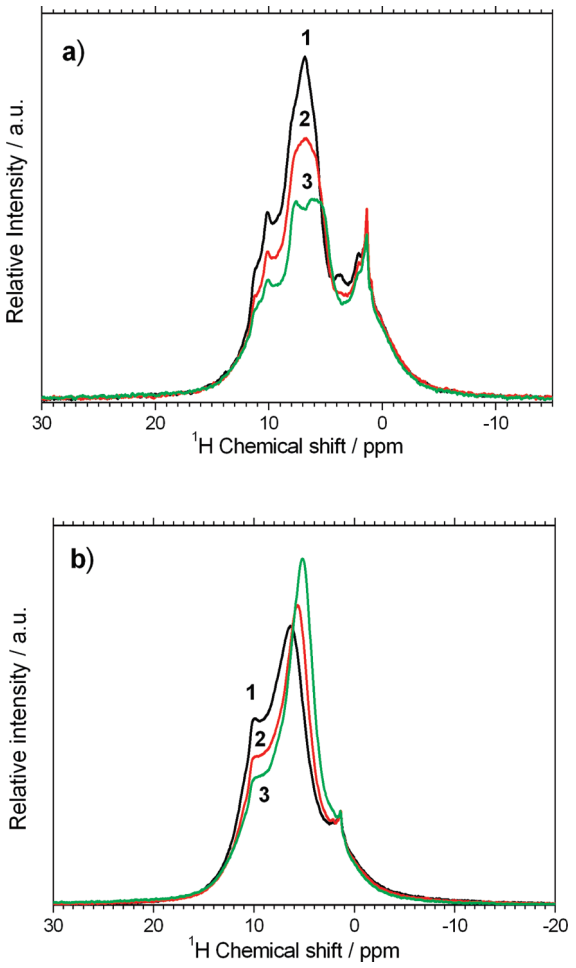

Figure 9. ^{1}H MAS NMR spectra of H-TiNT ion-exchanged with NaOH at (1) pH = 2, (2) pH = 9, and (3) pH = 13 followed by annealing at (a) 250 °C and (b) 140 °C for 24 h. Several peaks in the chemical shift region of 1.4 ppm are artifact signals from the NMR rotor.

ion-exchangeable protons, as well as an increase of the signal from crystallographic water at 5.7 ppm. These observations are in agreement with recent findings[44,45] that the sodium form of titanate nanotubes accumulates more crystallographic water. Hence, the sodium saturated form of the nanotubes has the approximate stoichiometry $Na_{1.4}H_{0.6}Ti_3O_7 \cdot 1.2H_2O$, whereas the protonated form of nanotubes can be approximated as $H_2Ti_3O_7 \cdot 0.2H_2O$.[45]

Supporting Information, Figure S4 shows ^{23}Na MAS NMR spectra of titanate nanotubes suspended at pH 2, 9, and 13, followed by drying at 140 °C. The spectrum has an asymmetrical shape. The spectra demonstrate successful ion-exchange of Na^+ ions in the titanate nanotubes following treatment at different pH values. The alteration of the amount of sodium in titanate nanotubes does not significantly affect the peak positions or peak shapes, suggesting minor changes in the ^{23}Na quadrupolar tensors for the three samples.

(44) Morgado, E., Jr.; Abreu, M. A. S.; Pravia, O. R. C.; Marinkovic, B. A.; Jardim, P. M.; Rizzo, F. C.; Araujo, A. S. *Solid State Sci.* **2006**, *8*, 888–900.
(45) Morgado, E., Jr.; Abreu, M. A. S.; Moure, G. T.; Marinkovic, B. A.; Jardim, P. M.; Araujo, A. S. *Mater. Res. Bull.* **2007**, *42*, 1748–1760.

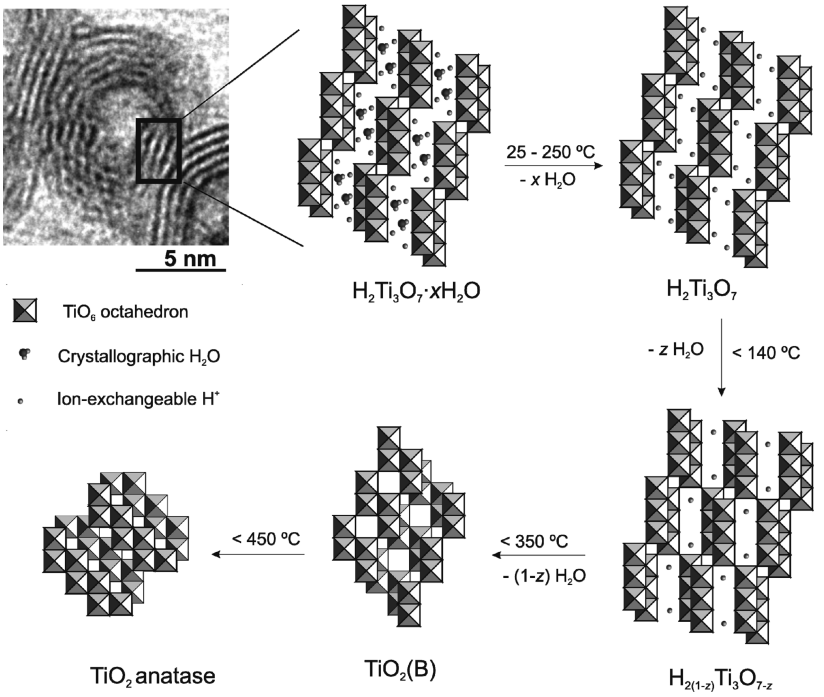

Figure 10. Modification of the crystallographic structure of protonated titanate nanotubes during their dehydration under thermal treatments. The black box in the HRTEM image of the nanotube cross-section (top left-hand side) indicates the corresponding fragment in its crystal structure.

Conclusions

In addition to the well established protons associated with physically adsorbed water,[17,31] two new types of protons namely, crystallographic water and ion-exchangeable protons of structural OH groups incorporated into the structure of titanate nanotubes, have been identified using MAS NMR techniques and standard structural methods (HRTEM, Raman spectroscopy, XRD, and TGA). The thermal treatment of H-TiNT results in their dehydration accompanied with structural and morphological transformation according to the sequence in Figure 10. The loss of crystallographic water occurs reversibly over a wide range of temperature according to

$$H_2Ti_3O_7 \cdot xH_2O \leftarrow \rightarrow H_2Ti_3O_7 + xH_2O \qquad (3)$$

. At 250 °C, almost all crystallographic water is lost. The addition of sodium ions into the structure of titanates results in an increase in the crystallographic water, that is, the stoichiometric coefficient x, but it does not prevent its disappearance at temperatures higher than 250 °C (see Figure 8a). The chemical shift of crystallographic water protons is at 5.7 ppm.

The combination of structural ion-exchangeable OH groups of titanate nanotubes also occurs over a wide range of temperature (starting below 140 °C) and resulting in dehydration. This, in turn, changes the stoichiometry of trititanates, according to

$$H_2Ti_3O_7 \rightarrow H_{2(1-z)}Ti_3O_{7-z} + zH_2O \qquad (4)$$

This dehydration is irreversible and decreases the ion-exchange capacity of nanotubes. The combination of OH groups in layered titanates may occur between OH groups from different layers resulting in a decrease of the gap between the layers via formation of structures with shared corner octahedrons (Figure 10). The intermediate cases may correspond to the various types of polytitanic acids including $H_2Ti_6O_{13}$ ($z = 0.5$) and $H_2Ti_{12}O_{25}$ ($z = 0.75$).[23] The NMR spectrum from ion-exchangeable protons is characterized by multiple peaks at 11.4, 10.0, 7.9, and 6.8 ppm. The rate of dehydration (which is stimulated by a high temperature) varies for different peaks, indicating their diverse nature.

Annealing at 350 °C removes almost all ion-exchangeable protons and transforms the crystal structure of nanotubes to the structure of monoclinic TiO_2 (B). A further increase in the temperature results in collapse of the tubular structure with formation of anatase nanorods.

Acknowledgment. The authors gratefully acknowledge financial support from the EPSRC, U.K. (Grant EP/F044445/1: "A hydrothermal route to metal oxide nanotubes: synthesis and energy conversion applications"). M.C. acknowledges the Royal Society University Research Fellowship scheme for financial support and Professor M. Levitt for the shared use of the NMR instruments.

Supporting Information Available: Figures S1−S4 and Table S1. This material is available free of charge via the Internet at http://pubs.acs.org.